

## Time-resolved magnetospectroscopy of $\text{In}_x\text{Ga}_{1-x}\text{As}/\text{GaAs}$ V-shaped quantum wires

M. Lomascolo,\* M. Anni, M. De Giorgi, R. Rinaldi, A. Passaseo, and R. Cingolani  
*INFN–Dipartimento di Ingegneria dell’Innovazione, Università di Lecce, I-73100 Lecce, Italy*

A. Lorenzoni and L.C. Andreani

*INFN–Dipartimento di Fisica “A. Volta,” Università di Pavia, I-27100 Pavia, Italy*

(Received 5 August 1999; revised manuscript received 15 December 1999)

We present a continuous-wave and time-resolved magnetoluminescence investigation of  $\text{In}_x\text{Ga}_{1-x}\text{As}$  V-shaped quantum wires (QWR’s) with In content  $x=0.1, 0.15, 0.2$ . The diamagnetic shifts and the field dependence (up to 8 T) of the recombination lifetime show a competition between exciton and free-carrier processes. In QWR’s with low In content ( $x=0.1$ ) the observed increase of the photoluminescence decay time with the magnetic field is explained by a theoretical calculation of free-carrier recombination. In-rich QWR’s exhibit instead a decrease of the decay time at low temperature, which is characteristic of the exciton recombination, and an increase at high temperatures when thermal ionization of excitons occurs. Our results indicate that the extent to which exciton or free-carrier recombination predominates depends on the temperature and on the strength of the built-in piezoelectric field.

The interplay between exciton and free-carrier recombination in quantum wires has been strongly debated in the literature.<sup>1–6</sup> This issue is important not only from the fundamental point of view, but also in view of the possible occurrence of excitonic lasing in quantum wire devices.<sup>4–6</sup> In strained  $\text{In}_x\text{Ga}_{1-x}\text{As}/\text{GaAs}$  V-shaped quantum wires (QWR’s) the assessment of the actual recombination mechanism is further complicated by the existence of a strong piezoelectric field at the high-index surfaces, which modifies the Coulomb interaction and reduces the exciton stability through the quantum confined Stark effect.<sup>7</sup> In this paper we present a continuous-wave and time-resolved magnetoluminescence investigation (up to 8 T) of  $\text{In}_x\text{Ga}_{1-x}\text{As}/\text{GaAs}$  V-shaped QWR’s as a function of the temperature and applied magnetic field. We demonstrate that samples with relatively high In content ( $x=0.15$  and  $x=0.20$ ) having deep lateral confinement potential up to 110 meV, exhibit dominant excitonic recombination at low temperatures. This manifests itself by a decrease of the radiative lifetime of the luminescence with increasing magnetic field. On the contrary, samples characterized by shallow lateral confinement potential (about 55 meV in the  $x=0.10$ ) exhibit an increase of the photoluminescence (PL) decay time with increasing magnetic field, which is demonstrated to be characteristic of free-carrier recombination. A calculation of the interband spontaneous radiative recombination rate as a function of the magnetic field shows that this effect is due to a flattening of the subband dispersion  $\epsilon(k_z)$  (where  $k_z$  is the wave vector along the wire axis) induced by the field.

A set of high-quality  $\text{In}_x\text{Ga}_{1-x}\text{As}/\text{GaAs}$  QWR’s was fabricated by metal-organic chemical vapor deposition on V-groove patterned GaAs substrates with (111) sidewalls. The pattern periodicity was 500 nm, the groove depth 250 nm. The samples were characterized by transmission electron microscopy (TEM).<sup>10</sup> The wires had identical shape and size, and the indium content  $x$  was varied between 0.1 and 0.2, in order to tailor the confinement of the electron/hole wave functions at the bottom of the wire. As shown in the TEM

cross section of Fig. 1(a), the QWR forms in the tapered part at the bottom of the groove, whereas a lateral quantum wire and a planar quantum well form on the (111) sidewalls

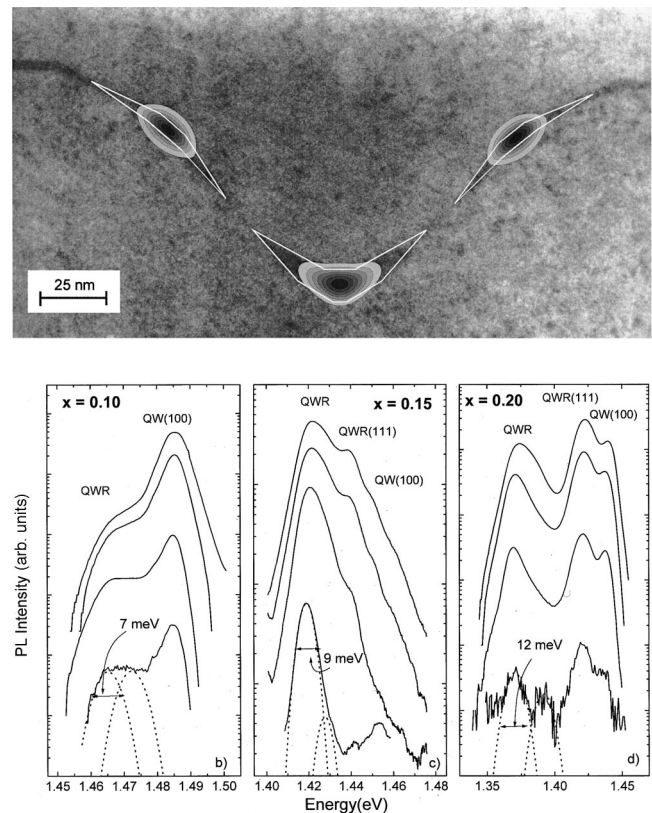


FIG. 1. (a) TEM cross section of a V-shaped quantum wire. The contour plots represents the theoretical electron ground level wave functions. (b)–(d) PL spectrum performed at 10 K at different excitation power intensity (continuous lines) of samples with different In content. The dotted lines represent the Gaussian deconvolution of the spectrum at low excitation intensity. Note that in the  $x=0.1$  sample the QWR(111) band is not resolved.

and in the region connecting adjacent wires [QWR(111) and QW(100), respectively]. Correspondingly, the low-temperature ( $T = 10$  K) PL spectra [Figs. 1(b)–1(d)] show three emission bands related to the QWR, QWR(111), and QW(100), at energy positions falling very close to those calculated by solving the two-dimensional Schrödinger equation with the potential profile obtained from the TEM cross section.<sup>10</sup> The photoluminescence FWHM (full width at half maximum) of the  $n = 1$  state obtained by a Gaussian deconvolution of the low excitation intensity spectra varies from 7 to 12 meV with increasing the In content, confirming the high quality of our samples. It is important to establish the role of disorder in the investigated samples, since strong localization effects have been reported by other groups.<sup>11–13</sup> Saturation of the localized luminescence is observed in Fig. 1 in the low-energy tail (around 1.355 eV for the  $x = 0.20$  sample and 1.455 eV for  $x = 0.10$ ) by increasing the power density from  $4 \text{ mW cm}^{-2}$  to  $10 \text{ W cm}^{-2}$  or under pulsed picosecond excitation: thus the fraction of localized excitations appears to be small, particularly for the  $x = 0.10$  and  $x = 0.15$  samples. The  $x = 0.20$  sample has greater localization and FWHM, due to increased alloy disorder.

The lateral extensions (full width at  $1/e$  maximum) of the ground and lowest excited state wave functions were found to be 20, 19, and 18 nm and 40, 36, and 34 nm for  $x = 0.1$ ,  $x = 0.15$ , and  $x = 0.2$ , respectively. Due to the different depth of the lateral potential and to the different strength of the internal piezoelectric field, the exciton stability is expected to depend appreciably on the In content. We have recently shown<sup>7</sup> that the enhancement of the exciton binding energy caused by the lateral confinement<sup>14</sup> is totally compensated by the Stark effect induced by the internal piezoelectric field in samples with low In content ( $x = 0.10$ ). In deeper QWR's, the piezoelectric field plays a minor role due to the larger confinement energy and to the decrease of the lateral wavefunction extension: thus the exciton is expected to have a higher stability in samples with  $x = 0.15$  and  $x = 0.20$ . This is indeed reflected in the diamagnetic shifts of the luminescence shown in Figs. 2(a)–2(c) for an excitation power density of about  $0.2 \text{ W cm}^{-2}$ . In the shallow QWR's ( $x = 0.10$ ), we observe a large quadratic shift at all temperatures, which agrees with the free-carrier diamagnetic shift calculated as described below. The shift amounts to about 4.5 meV at  $B = 8$  T, as opposed to about 1 meV for the exciton diamagnetic shift. The deeper QWR's ( $x = 0.15$  and  $0.20$ ) are found instead to be very sensitive to the lattice temperature in the range 4–90 K. At 4 K these samples exhibit a vanishing diamagnetic shift in the range 0–8 T [closed squares in Figs. 2(b) and 2(c)]. It should be mentioned that within the resolution (about 1 meV) achieved in the low-power density experiments the diamagnetic shift of free and localized exciton cannot be distinguished, the diamagnetic shift of free-exciton being about 1.5 meV at 8 T.<sup>14,11</sup> At  $T = 50$  K the luminescence recovers a large diamagnetic shift of about 3.5 meV for  $x = 0.20$  and 4 meV for  $x = 0.15$  at 8 T, indicating that excitons are thermally ionized.

These results suggest that exciton recombination is predominant in the deep quantum wires at low temperature, whereas free-carrier recombination is the main emission process in the shallow wires. This information is crucial for the discussion of the transient dynamics of the recombination in

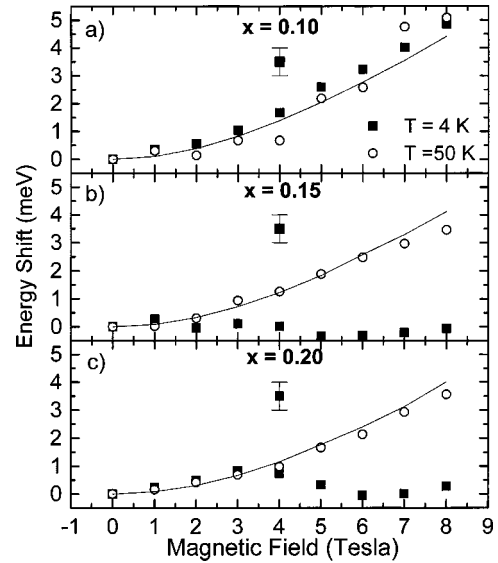


FIG. 2. Diamagnetic shift of  $\text{In}_x\text{Ga}_{1-x}\text{As}/\text{GaAs}$  QWR's with In content  $x = 0.10$  (a),  $x = 0.15$  (b), and  $x = 0.20$  (c) at different temperatures. Solid lines: theory.

high magnetic field. Time-resolved PL experiments at different temperatures were performed as a function of the magnetic field in the samples with  $x = 0.10$  and  $x = 0.15$ , the luminescence of sample  $x = 0.20$  being outside the detection range of our streak camera. Representative transient PL spectra of the  $x = 0.15$  sample at  $B = 0$  are shown in Fig. 3(a), for the planar QW(100), the lateral QWR(111), and the ground

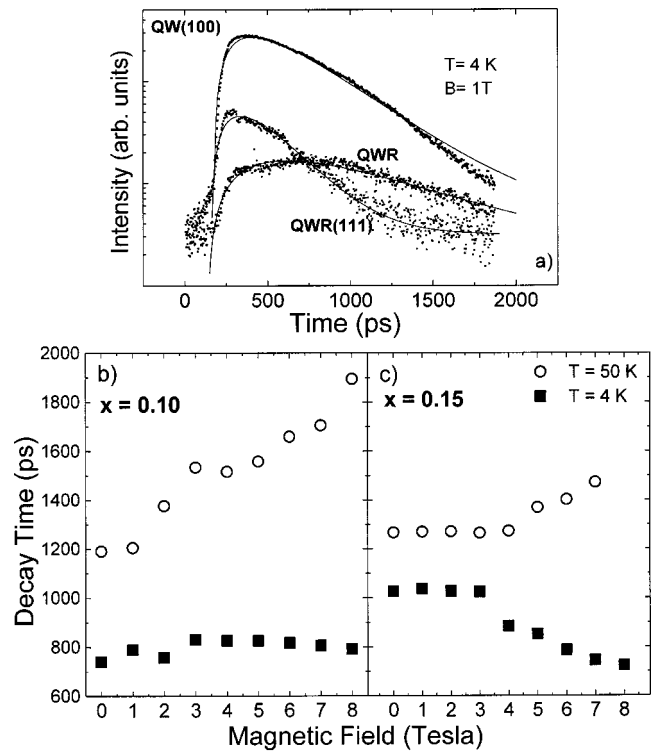


FIG. 3. (a) Time-resolved PL for the QWR's with In content  $x = 0.15$ . The continuous lines represent the best fit to the experimental traces by a three-level model. (b) and (c) Decay times versus magnetic field, as obtained from the fit of time resolved luminescence, for the  $x = 0.10$  and  $x = 0.15$  samples.

state (QWR). The continuous lines through the experimental traces are the best fit to a three level rate equation model,<sup>15,16</sup> which was used to extract the decay times from the spectra. In Figs. 3(b) and 3(c) we report the PL time constants obtained by the fit at different lattice temperatures, as a function of the magnetic field. The integrated PL intensity as function of temperature is constant up to about 60–80 K depending on the investigated samples, suggesting that in this range of temperature the time constants obtained by the fits refer to the radiative lifetime  $\tau_0$ .<sup>3</sup> The rise time is of the order of 50–200 ps in all the investigated samples and it is found to increase weakly with the magnetic field. On the other hand, the decay time exhibits different behavior with increasing magnetic field, depending on the  $x$  content.

In shallow quantum wires [ $x=0.1$ , Fig. 3(b)] the PL decay time at low temperature slightly increases with increasing magnetic field (from 730 ps at  $B=0$  T to 830 ps at higher field). This increase becomes more pronounced above 50 K, resulting in a change of about 60% of the zero-field lifetime. A similar relative change is observed at 70 K, even though the activation of nonradiative recombination channels starts to reduce the total PL decay time. In deeper quantum wires [ $x=0.15$ , Fig. 3(c)] we observe that in the range 4–50 K the PL decay time is constant for magnetic fields up to 3 T (about 1000 ps and 1400 ps at 4 K and 50 K, respectively). For magnetic fields larger than 3 T, we observe two different behaviors depending on temperature: at 4 K, the decay time decreases with increasing the magnetic field, whereas above 50 K it increases (from 1300 ps to 1500 ps).

These results suggest that different recombination mechanisms occur in our QWR's. In what follows we will explain the experimental results of Fig. 3 by a theoretical analysis of the exciton and free-carrier lifetime in the magnetic field. In the case of exciton radiative recombination, the effect of the magnetic field is to squeeze the electron-hole wave function in the plane perpendicular to the field. This results in three main effects: (i) a decrease of the lateral extension of the exciton wave function, (ii) an increase of the coherence area, which is proportional to the exciton dephasing time, and (iii) an increase of the oscillator strength, due to the larger probability to find the electron-hole pair closer in the same area.<sup>8,9,17</sup> These effects cause a reduction of the exciton decay time when the magnetic length is smaller than the lateral extent of the exciton wave function. The decrease of the PL decay time observed in the  $x=0.15$  sample at low temperature [Fig. 3(c)] is thus explained by an excitonic recombination.<sup>18</sup> When the exciton is ionized the field dependence of the PL decay time becomes free-carrier-like. This is actually the case in the  $x=0.10$  sample, where the shallow lateral potential and the piezoelectric field reduce the binding energy, and in the  $x=0.15$  sample above 50 K, when thermal ionization occurs.

In order to model the quantum wire in a magnetic field, we solved the effective-mass Hamiltonian within the envelope function approach. Assuming a wire axis along  $z$  and a constant magnetic field along the growth ( $y$ ) direction the Hamiltonian in the Landau gauge becomes

$$H = \frac{p_x^2 + p_y^2}{2m^*} + \frac{1}{2}m^*\omega_c^{*2}(x - l^2k_z)^2 + V(x, y), \quad (1)$$

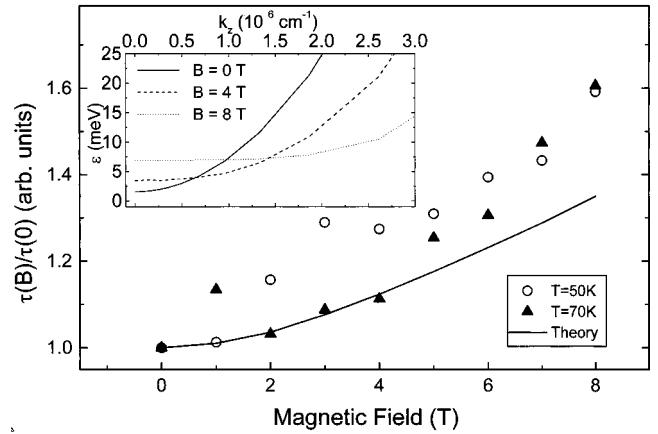


FIG. 4. Decay time as a function of magnetic field, normalized to the value at zero field, for the  $x=0.10$  QWR. Symbols: experimental results at two different temperatures. Solid line: theoretical results at  $T=50$  K. Inset: dispersion of the lowest QWR subband for three different values of the magnetic field.

where  $\omega_c^* = eB_0/m^*$  is the cyclotron frequency and  $l = \sqrt{\hbar/eB_0}$  is the magnetic length. We assume a rectangular cross section for the wire, of area equal to that of the actual samples. This leads to a decoupling of the Hamiltonian in two one-dimensional problems. The calculation including the shape of the potential as obtained from TEM is the subject of a forthcoming paper.

The effect of the magnetic field on the subband dispersion  $\epsilon(k_z)$  is twofold (see inset of Fig. 4): first, the energy at  $k_z=0$  has a quadratic diamagnetic shift. Second, the magnetic field induces a flattening of the dispersion curves. From a classical point of view this arises from the formation of cyclotron orbits that are completely contained inside the wire profile and that are centered at different positions  $x_0 = l^2k_z$ ; in the quantum-mechanical picture, Landau levels are formed, whose degeneracy corresponds to the flat region of the dispersion. The diamagnetic shift is approximately given by

$$\Delta E^{dia} \approx \frac{1}{2} e^2 B_0^2 \langle x^2 \rangle \left( \frac{1}{m_c^*} + \frac{1}{m_v^*} \right), \quad (2)$$

and is dominated by the carrier with the lighter mass.

In order to calculate the interband recombination lifetime for free carriers, we follow the theory of Bebb and Williams<sup>19</sup> developed for nondegenerate semiconductors. The radiative recombination rate per unit wire length is expressed in terms of the subband dispersion as

$$R_{sp} = A \sum_{ij, k_z} | \langle f_{ik_z}^c | f_{jk_z}^v \rangle |^2 e^{-[E_i^c(k_z) - \mu_c]/KT} e^{-[\mu_v - E_j^v(k_z)]/KT}, \quad (3)$$

where the constant  $A = 2e^2 n_r E_g |p_{cv}|^2 / (4\pi\epsilon_0 m^2 c^3 \hbar^2)$ ,  $|f_{ik_z}^c\rangle, |f_{jk_z}^v\rangle$  are envelope functions of conduction and valence subbands and  $\mu_c, \mu_v$  are chemical potentials.  $R_{sp}$  is proportional to the carrier densities  $n$  and  $p$  in conduction and valence bands. The recombination lifetime is given by  $\tau = 1/(B_{sp}n)$ , where  $B_{sp} = R_{sp}/np$  (for optical excitation  $n=p$ ). A similar treatment has been given for quantum

wells.<sup>20</sup> In the absence of a magnetic field and considering a single pair of subbands we obtain

$$\tau = \frac{1}{An} \left( \frac{(m_c^* + m_v^*)KT}{2\pi\hbar^2} \right)^{1/2}. \quad (4)$$

The radiative lifetime is dominated by the carrier with the heavier mass.

For nonzero magnetic field the expression (3) has been evaluated numerically. Since we are mainly interested in the magnetic field dependence of the lifetime, we divide by its zero-field value: the quantity  $\tau(B)/\tau(0)$  is independent of the carrier density.<sup>21</sup> The free-carrier recombination lifetime is found to increase with increasing field. This effect follows from the modified subbands dispersion: the flattening causes an increase in the density of states of carriers near the subband edges. Since the recombination lifetime is proportional to the density of states, as in Eq. (4),  $\tau$  increases with the field. Comparison with experiments shows good agreement for an In content  $x=0.1$  at a temperature  $T=50$  K (Fig. 4), confirming the free-carrier nature of the process as deduced from the diamagnetic shift. At  $T=4$  K the situation is quite different: on one hand we have evidence of free-carrier processes from the diamagnetic shifts [Fig. 2(a)], while on the other hand the radiative lifetime is almost field independent. This fact could be explained assuming that conduction band states are free, whereas valence-band states, which are heavier, are localized at  $T=4$  K. Within this picture, Eq. (2)

accounts for the high diamagnetic shifts, since the dominant contribution arises from conduction-band states. On the other hand, Eq. (4) shows that the radiative lifetime is dominated by the valence band states: in the limit of localized holes, the radiative recombination is like a free-to-bound transition,<sup>19</sup> and the lifetime does not depend on the field.

In conclusion we have investigated the competition between exciton and free-carrier recombination mechanisms by means of magneto-optical time-resolved photoluminescence. In QWR's with low In content ( $x=0.1$ ) at  $T=50$  K, the PL decay time increases with increasing the magnetic field. This behavior has been modeled on the basis of a theoretical calculation of the free-carrier interband recombination rate. On the other hand, In-rich QWR's exhibit a decrease of the decay time at low temperature, which is characteristic of the exciton recombination, and an increase at high temperatures when thermal ionization of excitons occurs. Our results indicate that the extent to which exciton or free-carrier recombination predominates at different temperatures, depends on the depth of the lateral potential and on the strength of the built-in piezoelectric field.

This work was supported by MURST, 40% Physics of Nanostructures, and TMR European Research Network: Ultrafast Quantum Optoelectronics. We gratefully acknowledge the expert technical help of D. Cannoletta and A. Melcarne.

\*Present address: CNR-IME, Via per Arnesano, 73100 Lecce, Italy.

<sup>1</sup>D.S. Citrin, Phys. Rev. B **47**, 3832 (1993).

<sup>2</sup>R. Cingolani, Phys. Scr. **T68**, 117 (1996).

<sup>3</sup>M. Lomascolo *et al.*, J. Appl. Phys. **83**, 302 (1998).

<sup>4</sup>W. Wegscheider *et al.*, Phys. Rev. Lett. **71**, 4071 (1993).

<sup>5</sup>H. Akiyama *et al.*, Phys. Rev. Lett. **72**, 924 (1994).

<sup>6</sup>R. Ambigapathy *et al.*, Phys. Rev. B **78**, 3579 (1997).

<sup>7</sup>R. Rinaldi *et al.*, J. Opt. Soc. Am. B **13**, 1031 (1996); M. Lomascolo *et al.*, J. Phys.: Condens. Matter **11**, 5989 (1999).

<sup>8</sup>M. Sugawara *et al.*, Phys. Rev. B **48**, 8848 (1993).

<sup>9</sup>I. Aksenov *et al.*, Phys. Rev. B **51**, 4278 (1995); **52**, 17 430 (1995).

<sup>10</sup>A. Passaseo *et al.*, J. Cryst. Growth **197**, 777 (1999).

<sup>11</sup>I. Rasnik *et al.*, Phys. Rev. B **58**, 9876 (1998).

<sup>12</sup>J. Bellessa *et al.*, Phys. Rev. B **58**, 9933 (1998)

<sup>13</sup>D. Oberli *et al.*, Phys. Rev. B **59**, 2910 (1999).

<sup>14</sup>R. Rinaldi *et al.*, Phys. Rev. B **53**, 13 710 (1996).

<sup>15</sup>G. Bastard, *Wave Mechanics Applied to Semiconductor Heterostructures* (Les Éditions de Physique, Les Ulis, 1988).

<sup>16</sup>Even though more accurate rate equation models could be adopted to describe the early 500 ps after the laser pulse (due to the very efficient carrier transfer among different levels of the structure), we found that for long delays the decay curve is governed mainly by the radiative recombination. In this case the simple three level model is expected to give a good approximation of the decay time constant.

<sup>17</sup>M. Lomascolo *et al.*, Appl. Phys. Lett. **74**, 676 (1999).

<sup>18</sup>The excitation intensity in the picosecond-time resolved experiments is rather high ( $>300$  W cm<sup>-2</sup>), so that the localized exciton states are saturated.

<sup>19</sup>H.B. Bebb and E.W. Williams, *Semiconductors and Semimetals* (Academic Press, 1972), Vol. 8.

<sup>20</sup>Y. Arakawa *et al.*, Appl. Phys. Lett. **46**, 519 (1985).

<sup>21</sup>Since  $A=2.9 \times 10^9$  s<sup>-1</sup> for GaAs, the measured lifetimes in the nanosecond range correspond to densities  $n \sim 2 \times 10^5$  cm<sup>-3</sup>.